Magnetic excitations in the itinerant ferromagnet UFe_2

L. Paolasini
European Commission, Joint Research Center, Institute for Transuranium Elements, Postfach 2340, D-76125 Karlsruhe, Federal Republic of Germany
and Département de Recherche Fondamentale sur la Matière Condensée, SPSMS/MDN, CEA-Grenoble, F-38054 Grenoble Cedex 9, France

G. H. Lander
European Commission, Joint Research Center, Institute for Transuranium Elements, Postfach 2340, D-76125 Karlsruhe, Federal Republic of Germany

S. M. Shapiro
Physics Department, Brookhaven National Laboratory, Upton, New York 11973

R. Caciuffo
Dipartimento di Scienze dei Materiali e della Terra, Università di Ancona, and Istituto Nazionale Fisica della Materia, Via Brecce Bianche, I-60131 Ancona, Italy

B. Lebech
Physics Department, Risø National Laboratory, DK-4000 Roskilde, Denmark

L.-P. Regnault
Département de Recherche Fondamentale sur la Matière Condensée, SPSMS/MDN, CEA-Grenoble, F-38054 Grenoble Cedex 9, France

B. Roessli
Institut Laue-Langevin, 156 X, F-38042 Grenoble Cedex, France

J-M. Fournier
Université J. Fourier, F-38000 Grenoble, France
(Received 10 January 1996; revised manuscript received 7 May 1996)

UFe_2 (Laves phase, fcc crystal structure) is a ferromagnet with $T_C=165$ K. Previous neutron elastic measurements have established that the Fe moment is $0.6\mu_B$ and that the moment on the U atom is almost zero because of the cancellation of the spin and orbital moments, which are both about $0.23\mu_B$, but are oppositely directed. We have now examined the spin dynamics from a large single crystal with both thermal and cold-source triple-axis spectrometers. Comparisons with the extensive work performed on $R\mathrm{Fe}_2$(R=Tb, Ho, Er) suggests that two dispersive modes should be seen at low energy (i.e., less than ~20 meV). However, only *one* mode has been found in UFe_2 and this involves the precession of the Fe spins. We propose that the acoustic mode involving the uranium spin is sufficiently broadened in ($\mathbf{q},\omega$) space that we cannot readily detect the excitation. Nevertheless, the influence of the U-Fe exchange may be seen in (a) the presence of a gap in the Fe spin-wave spectrum at $q=0$, and (b) in an *increase* in the Fe spin-wave stiffness constant (D) as compared to that found in pure Fe. This last property is a direct consequence of the hybridization between the U5f and Fe3d electrons. We find also that D is strongly temperature dependent, presumably due to two-magnon interactions. Thus, this effect, together with the low moment on the Fe atoms, results in the comparatively low, as compared to the $R\mathrm{Fe}_2$ compounds, T_C of 165 K in UFe_2. [S0163-1829(96)05234-4]

I. INTRODUCTION

The study of the spin waves of the $R\mathrm{Fe}_2$ (R=Tb, Ho, Er) cubic Laves phase compounds[1–7] has presented a clear picture of the microscopic magnetic exchange interactions in an alloy of Fe and a heavy rare earth. The principal result of these studies is that the interaction between the two magnetic species is relatively weak; the high Curie temperature T_C is provided by the Fe-Fe interactions, whereas the anisotropy is provided by the rare-earth ions.[8] Indeed, this separation of properties is behind the physics of technologically important materials such as the hard magnets $SmCo_5$, $Nd_2Fe_{14}B$, and amorphous $TbFe_2$. The magnetic anisotropy of the rare-earth ion contributes substantially to the coercivity, especially in uniaxial materials. Further details of the (weak-) coupling mechanism between the 4f and 3d electrons have emerged from local-density calculations,[9] and these illustrate the important role of the 5d electrons in being sensitive to the 4f moments and hybridizing with the 3d electrons. Theory and experiments are in good agreement, confirming that most

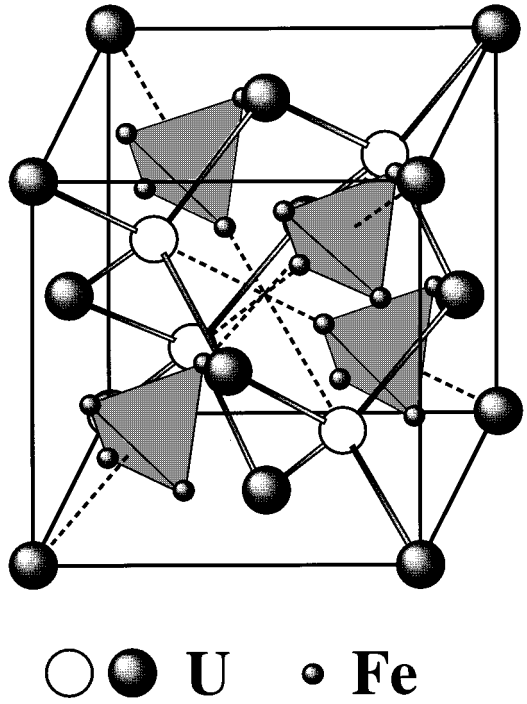

FIG. 1. Laves phase fcc cubic structure of the $R\mathrm{Fe}_2$ compounds. The larger spheres are R atoms, the smaller Fe. For the R atoms there are two Bravais lattices, each one being generated by the face-centering operator. Those based on the atoms at the origin (000) are shown as solid circles, those generated from the atom at (1/4,1/4,1/4) are shown as open circles. The Fe atoms are arranged in tetrahedra surrounding the (3/4,3/4,3/4) point and its symmetric equivalently related points.

magnetic properties can be explained by the ''standard model'' of rare-earth magnetism.[10]

Building on this well-established base we now pose the question what happens to the magnetic properties when the f-electron atom is replaced by Ce or U? (Unfortunately, the Pr and Nd compounds do not form in the cubic Laves phase.) Clearly, the situation is more complex, principally because the f electrons in these systems can exhibit a high degree of delocalization. As a result they can hybridize directly with the $3d$ electrons, rather than indirectly via the $5d$ electrons as in the cases discussed above. The face-centered-cubic Laves-phase structure (Fig. 1) is particularly interesting as it has short interatomic distances, thus providing opportunity for such direct hybridization when the f electrons are not localized. Some of the properties of the compounds discussed in this work are given in Table I. The Fe-Fe distance in this structure ($\sim$2.5 Å with coordination number 6) is actually shorter than that found in pure iron (2.8 Å with coordination number 8). The U-U separation (3.0 Å) in UFe_2 is also smaller than the Hill limit[11] of $\sim$3.4 Å. The most significant difference between the $R\mathrm{Fe}_2$ compounds on the one hand, and CeFe_2 and UFe_2 on the other, is that the Ce and U compounds have much lower T_C's and smaller moments on the f sites. It should be emphasized that the absence of a moment on the R site does not imply a small T_C. Both YFe_2 and LuFe_2 have high values of T_C. It is the interaction between the f and $3d$ electrons that appears to be the key factor in reducing T_C.

For CeFe_2 the possibility of strong hybridization effects was first discussed by Eriksson *et al.*[12] Unfortunately, the experimental situation in CeFe_2 is not clear as recent reports of neutron elastic[13] and dichroism[14] measurements are not in agreement with one another on the magnitudes of the moments at the two sites. More work is required to understand CeFe_2.

In the case of UFe_2 a number of studies have been undertaken. Aldred[15] summarized the earlier work and showed that the material is a ferromagnet with a total moment of 1.09 μ_B/(formula unit) and rather small anisotropy. Andreev *et al.*[16] focused particularly on the small anisotropy, and concluded (as did Aldred[15]) that the $5f$ electrons of uranium must be largely itinerant. In apparent contradiction to the small *total* anisotropy, Popov *et al.*[17] showed that UFe_2 has a sizable rhombohedral distortion at T_C. The intrinsic strain (defined as the relative differences in length measured parallel and perpendicular to the rhombohedral axis) is $+4.5\times10^{-3}$. Whereas this is smaller than that found in $\mathrm{TbFe}_2(+8.6\times10^{-3})$ or $\mathrm{NpFe}_2(-12.0\times10^{-3})$, it is still almost 2 orders of magnitude greater than that found in Fe itself.[18] One would expect, therefore, to find considerable total anisotropy in UFe_2, because the distortion will contribute a sizable term (in the form of a strain anisotropy) to the total anisotropy. However, Popov *et al.*[17] showed that the small total value is due to an accidental cancellation of the magnetostrictive term λ_{111} (related directly through the c_{44} elastic constant to the strain anisotropy) with an almost equally large, but oppositely directed, term from the intrinsic anisotropy. In a further series of experiments Sorokina *et al.*[19] measured the elastic constants as a function of temperature and found a large softening of the c_{44} elastic constant near T_C. Eremenko *et al.*[20] ascribed this to a strong magnon-

TABLE I. Properties of the $R\mathrm{Fe}_2$ and UFe_2 compounds at $T=0$ K. Data on rare-earth compounds taken from Ref. 8, those from UFe_2 taken from Ref. 24. The heavy rare earths are assumed to have their full Russell-Saunders ground state. The quantities μ_{total}, μ_S, and μ_L are, respectively, the total, spin, and orbital magnetic moments of the rare-earth (or uranium) site [see Eq. (2)]. The final column gives the moments found on the Fe sites. The numbers in parentheses refer to standard deviations on the least-significant digit. The nearest R-R (or U-U) distance in the structure is given by $(\sqrt{3}/4)a_0=0.433a_0$ and the nearest Fe-Fe distance is given by $(\sqrt{2}/4)a_0=0.3536a_0$.

$R\mathrm{Fe}_2$	a_0 (Å)	T_C (K)	Easy axis	μ_{total} (μ_B)	μ_S (μ_B)	μ_L (μ_B)	μ (Fe) (μ_B)
TbFe_2	7.348	705	$\langle111\rangle$	9.0	6.0	3.0	1.5
HoFe_2	7.301	614	$\langle100\rangle$	10.0	4.0	6.0	1.5
ErFe_2	7.276	596	$\langle111\rangle$	9.0	3.0	6.0	1.5
UFe_2	7.057	165	$\langle111\rangle$	0.01	$-0.22(1)$	$+0.23(1)$	0.60(5)

phonon interaction. Mössbauer experiments were also interpreted[21] as showing that UFe_2 is anomalous in comparison with the other rare-earth Fe_2 Laves phases as, in the case of UFe_2, the Lamb-Mössbauer factor suddenly increased at T_C. We shall return to all of these points later in this paper, but previous studies do show that UFe_2 has unusual properties.

Evidence for strong hybridization in UFe_2 between the U $5f$ and Fe $3d$ electrons was first provided by Brooks *et al.*[22] in a theoretical paper. They predicted that one consequence of the hybridization would be a reduction, as compared to the free-ion value, in the orbital moment on the uranium. Using polarized neutrons and elastic scattering Wulff *et al.*[23] and Lebech *et al.*[24] showed that this was, in fact, the case. The orbital and spin moments are both about $0.25\mu_B$, but they are oppositely directed, and hence the net moment, which is the sum of the orbital and spin contributions, on the U site is close to zero. For a ''normal'' $5f^3$ configuration we would expect[25] the ratio of orbital to spin (μ_L/μ_S) to be about -2.5 so that the absolute magnitude of this ratio is strongly reduced (to ~ 1.0) in UFe_2. It should be appreciated that, from a theoretical point of view, the AFe_2 series (A=U, Np, Pu, and Am) are best treated as itinerant systems with a large orbital moment.[26] The neutron experiments[23,24] on single crystals of UFe_2 also showed that the Fe moment was $0.60\pm 0.03\mu_B$, a substantial reduction from the $2.2\mu_B$ of pure Fe, or the $1.5\mu_B$ found on Fe in the RFe_2 series (Table I). The total moment in UFe_2 is then $2\times 0.60+(\sim 0)=1.2\mu_B$ per formula unit, and the magnetization results of $\sim 1.1\mu_B$ (depending on the exact stoichiometry) show that, as expected, the conduction-electron polarization is oppositely directed to the Fe $3d$ moment.[9]

No measurements of spin dynamics or phonons have been reported in UFe_2. Our motivation for these experiments was to examine how the hybridization between the $5f$ electrons of uranium and the $3d$ electrons of iron affects the magnetic exchange parameters and spin-wave spectra. These effects are considerable.

II. SPIN DYNAMICS OF RFe_2 SYSTEMS

The formalism for interpreting the experiments[1–7] on the RFe_2 compounds has been developed and is particularly clearly given in Clausen *et al.*[6] Figure 2 shows the three spin-wave branches we expect at low energy. There are three additional modes involving optic vibrations of Fe atoms, but they are too high in energy to be observed easily, although some attempts have been reported on isostructural $HoCo_2$.[27] The acoustic mode (1) involves both R and Fe spins precessing in phase. Mode (2) involves the precession of the Fe spins only. This mode can be thought of as very similar to that appearing in pure Fe. Mode (3) involves the energy of the rare-earth ion making a precessional motion in the molecular field established by the Fe atoms. Following the theory for the RFe_2 compounds, the energies of modes (2) and (3) at $q=0$ (i.e., the gaps in the spectra) are given by

$$\Delta E_2 = 12\mathcal{J}_{R\text{-Fe}}(S_R - 2S_{\text{Fe}}),$$
$$\Delta E_3 = 24 S_{\text{Fe}}\mathcal{J}_{R\text{-Fe}} \qquad (1)$$

where $\mathcal{J}_{R\text{-Fe}}$ is the R-Fe exchange energy and S_R, S_{Fe} are spins of the rare-earth atom and iron, respectively. The total

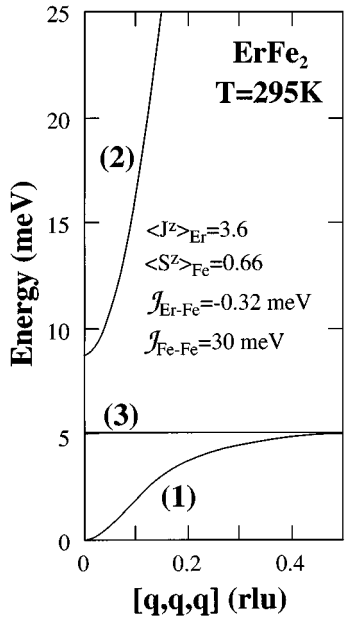

FIG. 2. The spin waves in $ErFe_2$ at 295 K ($\sim 0.5T_C$) as a function of wave vector in the $\langle 111\rangle$ direction, taken from Refs. 2, 5, and 6. These are representative of the low-energy ($E<30$ meV) modes in all the heavy rare-earth RFe_2 series. Modes (1), (2), and (3) are discussed in the text.

anisotropy is related to both the energies ΔE_1 and ΔE_2. In Fig. 2, E_1 is shown with no gap, but one develops in the RFe_2 compounds at low temperatures. Note that we have neglected crystal-field interactions at the rare-earth site. Since the molecular exchange field of the Fe on the R atom is strong the $|M_J\rangle = |J\rangle$ ground state of the R atom gives the ground-state wave function and mode (3) is a measure of energy needed to populate the $|M_J - 1\rangle$ state. Due to the strong exchange the R atoms have their full moments, so other states at higher energy are not accessible with dipole transitions. In some rare-earth systems, particularly when the transition element is cobalt, a small crystal-field exists,[4,5,27,28] but as we observe no dispersionless modes, such as (3), in UFe_2 we shall not discuss crystal-field effects. It is worth noting at this stage that the intensity of mode (3) will be proportional[28] to the square of the spin of the R (or U) atom. Since the spin is so much smaller in the case of the U atom than for a heavy rare-earth, the intensity of mode (3) may well be small, even if it exists.

Equation (1) above contains an important change from the formulas as written in the papers on isostructural rare-earth compounds. We have replaced J, the total angular momentum, by the total spin S. In the equations of motion the spin is the relevant quantity, but, in the localized $4f$ series, the spin S and orbital L momenta are coupled together via Russell-Saunders relationship, so that we usually write J in the formula as the neutron dipole selection rules for transverse spin waves involve $\langle M_J \pm 1\rangle$ operators. We recall

$$\mu_{\text{total}} = gJ,$$
$$\mu_S = 2(g-1)J,$$
$$\mu_L = (2-g)J, \qquad (2)$$

where g is the Landé factor. In a system with a quenched ($L=0$) orbital moment $g\sim 2.0$, and the orbital moment is zero. This is not the case in UFe_2. On the other hand, the ratio μ_L/μ_S is far from that expected for a localized rare-earth ion in UFe_2.

The lack of dispersion in mode (3) is a consequence of the weak exchange $\mathcal{J}_{R\text{-Fe}}$. In the RFe_2 systems this is some 2 orders of magnitude less than $\mathcal{J}_{\text{Fe-Fe}}$. Whereas this interaction in UFe_2 might be expected to be greater, because of the direct hybridization, we can certainly still expect $\mathcal{J}_{\text{Fe-Fe}} \gg \mathcal{J}_{\text{U-Fe}}$. The strong dispersion in mode (2) arises from the Fe-Fe interaction $\mathcal{J}_{\text{Fe-Fe}}$, which gives a dispersion of this Fe mode similar to that measured in pure iron. We can easily evaluate experimentally the spin-wave stiffness D for RFe_2 in the relation

$$E_2=\Delta E_2+Dq^2, \tag{3}$$

and show that observed values $D(RFe_2)\sim D(\text{Fe})\sim 300$ meV Å^2, and that these values are almost independent of temperature. Note that we have assumed the R-R interaction, $\mathcal{J}_{R\text{-}R}$, is negligible. Whether this is valid also in UFe_2 is unknown.

III. EXPERIMENTAL DETAILS

A. Sample

All measurements have been performed on a single crystal of UFe_2 grown by the Czochralski technique at CEN-Grenoble. Not all the original crystal was single, and in view of the twinning problems encountered[24] in the diffraction experiments on a different UFe_2 crystal, considerable care was taken to characterize the crystal in detail. Neutron Laue photographs, taken at the Laboratoire Léon-Brillouin, Saclay, France showed that a small part of the end of the original crystal was not single, and this was removed. The crystal dimensions are ~6 mm diameter, with a length of 33 mm. ac-susceptibility and resistivity measurements showed that the crystal becomes ferromagnetic at 165.5 K. This is close to the value of 167 K established by Aldred as the T_C of stoichiometric UFe_2. In none of the neutron experiments described below did we find any evidence of additional Bragg peaks or satellites at low temperature. All evidence confirms that our crystal is single, close to stoichiometry, and that UFe_2 is a ferromagnet.

B. Neutron experiments

These were performed on thermal triple-axis spectrometers at Siloë (CEN-G, Grenoble) and at the High-Flux Beam Reactor at Brookhaven National Laboratory. In addition, triple-axis spectrometers at the cold sources at Risø National Laboratory, Denmark, and at the Institut Laue Langevin (ILL), Grenoble, France, were used.

For the thermal spectrometers most of the experiments were taken with k_f fixed (BNL) or k_i fixed (Siloë) at 2.62 Å^{-1} (14.3 meV) and a pyrolytic graphite filter in the appropriate place to reduce second-order contamination. Some experiments were also performed (at Siloë) with $k_i=4.1$ Å^{-1} (34.8 meV) to make constant-**Q** scans up to ~15 meV at low temperature. At the cold-source spectrometers $k_f=1.5$ Å^{-1} (4.6 meV) was used with a Be filter to eliminate higher-order contamination.

Pyrolytic graphite monochromators and analyzers were used throughout with moderate collimation (~40′). Because of the close proximity of most of the magnetic scattering to the zone center ($q=0$), particular care had to be taken in eliminating spurious phonons that arose either from the poor collimation, or from the vertical divergence introduced by a focusing monochromator. This was particularly true for the initial measurements made at Risø, which, although contaminated by phonon scattering, were the first to show conclusive evidence of inelastic magnetic scattering, and defined the region of ($\mathbf{q},\omega$) space that had to be examined. At the ILL the cold-source spectrometer[29] (IN14) was used with incident polarized neutrons from a bender and the analyzer was a Heusler crystal so full polarization analysis was possible. Flipping ratios were 9.6 at 100 K, and 11.2 at 50 K. This shows that there is a small depolarization of the beam, presumably from surface domains, at higher temperatures. The incident polarization corresponds to 0.81.

An experimental run was also made on the PRISMA time-of-flight crystal-analyzer spectrometer[30] at ISIS. No magnetic excitations could be observed at PRISMA, but the instrument was useful in mapping the optical phonons, see Sec. VI.

IV. RESULTS

A. Fe mode

Figure 3(a) shows the results of scans in the [111] direction at a constant energy transfer of 1.5 meV. Note that, despite the small value of $|\mathbf{Q}|=1.54$ Å^{-1}, the phonons can be seen easily at 300 K, including the transverse acoustic (TA) [111] phonon that would usually be ''forbidden'' as these scans are purely longitudinal. The phonon scattering may be scaled by the Bose factor and decreases substantially by ~150 K. The two spin waves $\pm\,\mathbf{q}$ on either side of the [111] position are seen at 50 and 100 K. At 150 K the spin wave shows broadness and even at 200 K can be identified, although the central part has now been ''filled in,'' corresponding to overdamped paramagnons. On the right-hand side, Fig. 3(b), is shown $\chi''(\mathbf{q},\omega)$. This shows clearly both the changing position of the peak in $\chi''(\mathbf{q}, E=1.5\text{ meV})$, as well as the presence of a signal above $T_C=165$ K. The spin waves up to ~100 K are resolution limited.

At higher-energy transfers, and thus larger values of q, the TA phonons are well separated from the magnetic modes, and focusing optics and wider collimation can be used. Nevertheless, the spin-wave intensity falls as $1/E$, so that with an Fe moment of $\sim 0.6\mu_B$ the experiments are difficult.

To determine which spins contribute to observed modes we use structure factor arguments. Table II gives the *elastic* structure factors for various Bragg reflections (zone centers). Figure 4 shows scans about three different reciprocal-lattice points with the sample temperature $T=100$ K. These three zones have different elastic structure factors. By far the smallest contribution from the phonons is found around the points such as (111). If we now turn to the magnetic signal, we may deduce that the signal comes only from the Fe mo-

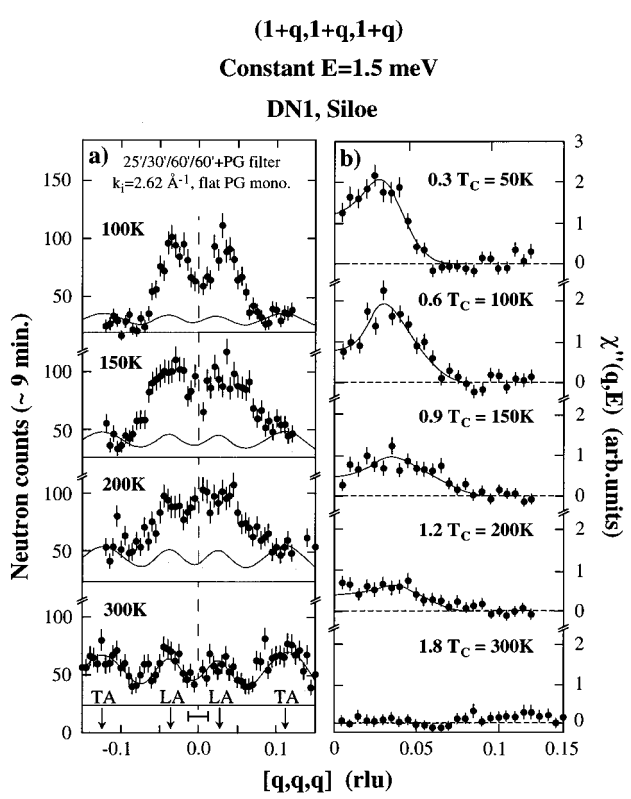

FIG. 3. (a) Neutron inelastic spectra taken at DN1 Siloë reactor with $k_i=2.62$ Å^{-1} (filter before sample) and with a neutron energy gain of 1.5 meV. The signals above background (~25 cts) at 300 K are from the phonons. At lower temperatures these are estimated by applying the Bose factors to the signal determined at 300 K, and are represented as shaded areas. The instrumental resolution in q space is shown as a horizontal bar in the lower panel. (b) The $\chi''(\mathbf{q},\omega)$ of the magnetic susceptibility [obtained by dividing the net magnetic signal in (a) by the Bose factor].

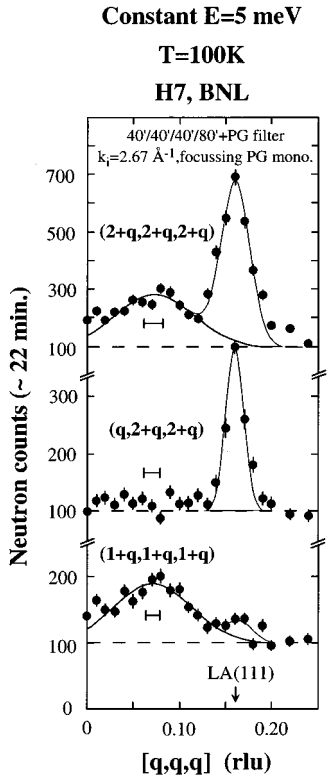

FIG. 4. Scans taken at HFBR Brookhaven (H7) with $k_i=2.67$ Å^{-1} (filter before sample) and with a neutron energy loss of 5 meV. The three scans are in the [111] direction with the sample at $T=100$ K, but from reciprocal-lattice points (222), (022), and (111) from top to bottom.

ments. This may be seen as follows. First, the elastic structure factor at the (022) contains U contributions only, but no magnetic scattering (center panel of Fig. 4) is seen around the (022). Second, using the structure factors for the (111) and (222) reflections, we can calculate the ratio of intensity

TABLE II. Elastic structure factors for the zone centers (Bragg points) for the fcc Laves phase in the zone (hkk), i.e., with an [1,−1,0] axis vertical as in the experiment. The geometric terms give the contribution of each species to the structure factor.

(hkk)	U	Fe
111	$-1/\sqrt{2}$	1
200	0	0
022	1	0
311	$+1/\sqrt{2}$	1
222	0	2
400	−1	2
133	$-1/\sqrt{2}$	1
422	1	0
044	+1	2

assuming that the contribution from the uranium is zero. Using a conventional Fe form factor, as found[24] for UFe_2, we find this ratio given by

$$I_{\text{magn}}(222)/I_{\text{magn}}(111)\sim 1.6,$$

which is consistent with the observed intensities in Fig. 4. Given our neglect of the dynamical structure factors, this agreement is remarkable, and, coupled with the absence of scattering at the (022), shows conclusively that the spin wave involves Fe spins only.

Turning to low energy we show in Fig. 5 data at a series of temperatures from the IN14 with complete polarization analysis. These data are reminiscent of Fig. 3 except that they show a larger change in the intensity of the spin wave near T_C (i.e., between 160 and 180 K), where the signal intensity decreases much faster than evident in Fig. 3. This can be understood by comparing the volume of the resolution ellipsoids for the two spectrometer configurations. It is approximately a factor of 30 times smaller with $k_i=1.5$ Å^{-1} (Fig. 5) than with $k_i=2.62$ Å^{-1} (Fig. 3). Thus, when the spin wave becomes broad, less weight is collected in the detector and it becomes difficult to observe the signal above the background. In contrast, below 100 K all experiments show that the Fe spin wave is resolution limited. In addition, the appearance of all the spin-wave intensity in the spin-flip channel shows that the spin wave is a conventional transversely polarized wave, since the neutron polarization is parallel to

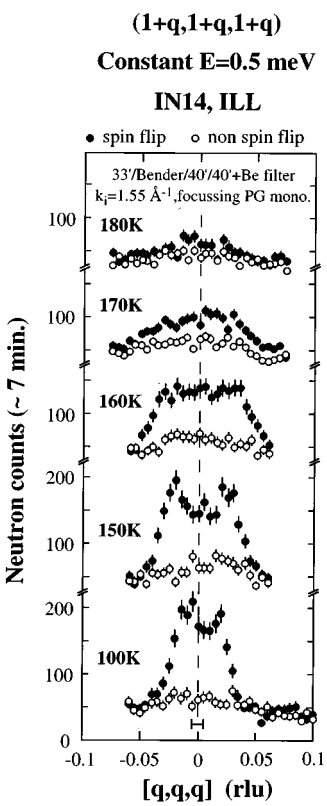

FIG. 5. Data taken with polarization analysis at IN14. The incident wave vector was $k_i=1.55$ Å^{-1}. A Be filter was used to suppress higher-order contamination and polarization was by a curved bender after focusing PG (002) monochromator. The analyzer is focusing Heusler. The polarization was 0.81. The data have not been corrected for incomplete polarization. A horizontal magnetic field of 1 T saturates the sample along the [111] direction. The energy transfer is 0.5 meV in neutron energy loss. The instrumental resolution in q space is shown as a horizontal bar in the lower panel. Solid points are spin-flip (i.e., magnetic) and open points are non-spin-flip (nonmagnetic).

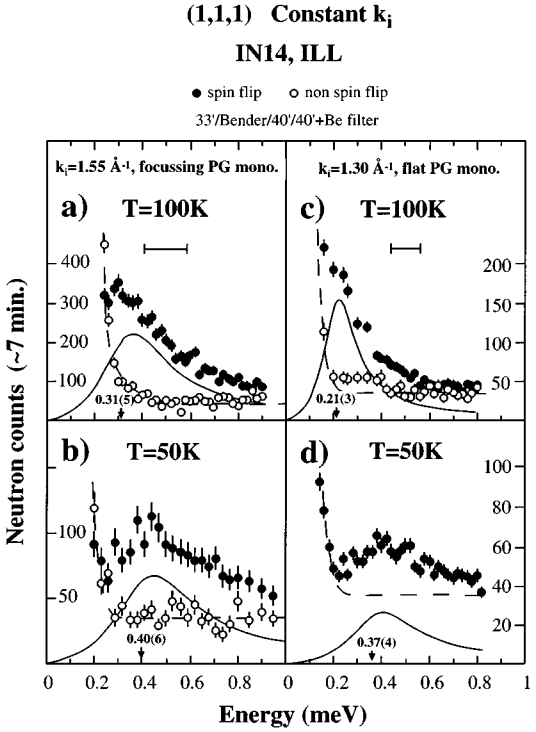

FIG. 6. Constant-**Q** scans at the (111) reciprocal-lattice point with IN14. (a) and (b) have the same experimental conditions as in Fig. 5(c) and (d). Incoming wave vector reduced to $k_i=1.3$ Å^{-1} and flat monochromator. The data here have been corrected for incomplete polarization. The dashed lines indicate background, the solid lines are the results of fits with an asymmetric Lorentzian form (see text) to determine the gaps in the magnetic spectra. The numbers above the energy axis give the results of these fits.

H$\|$ [111]. Scans in other directions have shown that the dispersion of the Fe mode is isotropic.

B. Measure of the gap in Fe mode

The polarized-neutron capability of IN14 has also been used to establish the gap in the Fe-spin-wave mode [ΔE_2 in Eq. (3)] at low energy. Data taken in constant **Q**=[111] are shown for two different configurations and temperatures in Figs. 6(a)–6(d). These data establish unambiguously that $\Delta E_2=0.39(2)$ meV at 50 K, and that it decreases considerably on warming to 100 K. Unfortunately, because of the large loss of intensity due to the Bose factor, this is difficult to measure near $T=0$. There is some inconsistency between the values with the focusing and flat monochromators, especially at $T=100$ K, and this may be due to resolution effects. With both configurations it is clear that ΔE_2 decreases as the temperature is increased. Note that the tail on these constant-**Q** scans is a resolution effect as the ellipsoid touches the sides of steeply rising dispersion curve. To simulate this effect we found empirically that adding a term proportional to the energy transfer, E, to the normal Lorentzian form was able to well represent the data. See the solid lines in Fig. 6. The resolution of IN14 is sufficiently good to avoid observing either the longitudinal or ''forbidden'' transverse acoustic phonons.

C. Search for additional modes

We have discussed at length the measurements of the Fe spin-wave for a good reason. No sign has been found of any other mode. This is an unexpected result, particularly with respect to mode (1) of Fig. 2. Proving that something is absent is, of course, difficult. That is one of the reasons we have used so many different spectrometers. In the process we have characterized the phonons of this material and made innumerable scans in (**Q**,ω) space, including constant-**Q** scans, sampling the first three Brillouin zones, and including a variety of zone-center and zone-boundary points. Since our present understanding (see Sec. V below) leads us to believe the acoustic mode involving Fe and U should lie below the Fe spin wave, we present in Fig. 7 three scans of interest, all with polarization analysis. Figure 7(a) shows that the transverse acoustic phonon is not a mixed magnon-phonon mode. Figure 7(b) shows a scan at lower energy than the Fe mode, but at small **q**, where any damping effects might be expected to be small. Figure 7(c) shows that no strongly overdamped magnetic mode contributes to the ($E\sim0$) incoherent scattering.

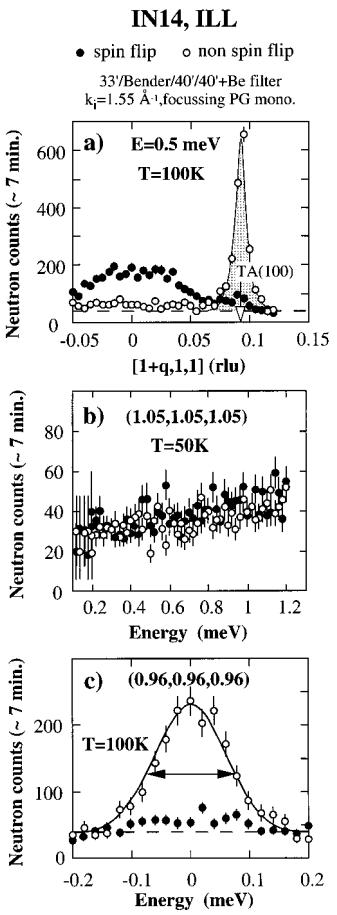

FIG. 7. Scans taken at IN14 with the same configuration as in Fig. 5. (a) Constant $E=0.5$ meV scan in direction [100] so as to intersect transverse acoustic (TA) phonon, (b) constant $\mathbf{Q}=[1.05,1.05,1.05]$, (c) constant $\mathbf{Q}=[0.96,0.96,0.96]$ showing incoherent non-spin-flip scattering. The calculated instrumental resolution is shown as a horizontal arrow. In all cases open points are non-spin-flip (nonmagnetic) and solid points are spin-flip (magnetic) scattering. Background levels are indicated as dashed lines.

These scans, and many others with spectrometers at BNL and Siloë, show the absence of any low-energy scattering up to ~10 meV, apart from the Fe mode. These statements are based on the assumption that any extra modes would be as sharp as the Fe modes, i.e., approximately resolution limited at low temperature.

V. ANALYSIS OF RESULTS

In Fig. 8 we present the dispersion of the Fe mode at $T=100$ K. In attempting to analyze this data we are at a considerable disadvantage. The theory we have discussed in Sec. II predicts three low-energy modes, and we have observed only one. First, this suggests the theory is inapplicable, or at best qualitative. Second, even if we follow the theory, we have too little information to solve for all the parameters. At this stage we shall use the theory of the $R\mathrm{Fe}_2$ systems as a guide, being aware of possible shortcomings.

We first note the expression for the Fe spin-wave gap in Eq. (1). If $S_U<2S_{Fe}$ there would be no gap in the spectrum of the Fe spin wave, or at least nothing greater than the gap

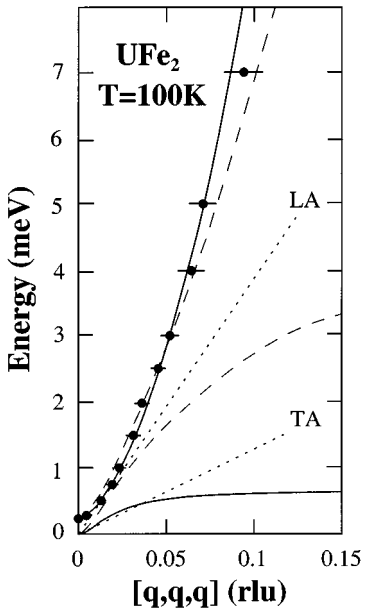

FIG. 8. Dispersion at $T=100$ K of the Fe mode (experimental points) together with transverse acoustic (TA) and longitudinal acoustic (LA) phonons marked as dotted curves. Two different analyses of the data discussed in the text are also presented on the graph. In each case the model predicts the Fe spin wave and an acoustic magnetic mode. These are marked as solid lines (model 1) and dashed lines (model 2), respectively, and the parameters are shown in Table III.

of less than 0.1 meV found in pure Fe,[31] instead the ''acoustic'' mode would have a gap and be at higher energy. So the finite gap in the Fe spin wave can be interpreted that $S_U>2S_{Fe}$. In our case at $T=100$ K the iron moment is $0.55\mu_B$ so $S_{Fe}=0.275\mu_B$, since the g factor for Fe is normally taken as 2. This inequality then gives $S_U>0.55\mu_B$. Recall that we have used S_U as an effective spin, in place of the normal J that occurs in the formula given for rare-earth materials. Recognizing that there is an orbital moment also associated with the uranium site, it is necessary to know the Landé factor g to obtain a value for the moment from this effective spin, see Eq. (2). It is exactly that value of g that is unknown in the case of uranium in UFe_2, since the polarized neutron experiments[23,24] have shown that μ_L and μ_S do not have the values expected from Russell-Saunders coupling. We cannot therefore relate the effective spin S_U found in the neutron inelastic experiments with the moment found in the elastic experiments but our analysis does show that a *nonzero* effective spin is required at the uranium site.

The formalism we have developed in Sec. II is valid for the case of a *localized* rare-earth ion interacting with Fe spins. All the evidence presented so far about UFe_2 shows that both the uranium and iron moments are *itinerant*. Thus, it is certainly not surprising that the predictions from the model of a localized model are not substantiated when (itinerant) uranium moments are involved. However, it is surprising that we have been unable to find the acoustic mode of the elementary magnetic excitations, because this should involve contributions from both moments.

The iron spin-wave mode may be modeled with the formalism of Sec. II. The parameters required are S_{Fe}, S_U,

TABLE III. Microscopic parameters used in the analysis of the inelastic scattering from the $R\mathrm{Fe}_2$ systems. The parameters for the $R\mathrm{Fe}_2$ systems correspond to $T=295$ K ($\sim 0.5T_C$) and have been collected from Refs. 1–7. The parameters for UFe_2 correspond to $T=100$ K ($0.6T_C$) S_{Fe} corresponds to the Fe spin, assuming $g_{\mathrm{Fe}}=2$. The column J_R corresponds to the total angular momentum in the case of the rare earths, but the ''effective spin'' in the case of UFe_2. The fits to the data for models 1 and 2 are shown in Fig. 8. The numbers in parentheses refer to standard deviations on the least-significant digit.

$R\mathrm{Fe}_2$	S_{Fe} (μ_B)	J_R (μ_B)	ΔE_2 (meV)	$\mathcal{J}_{\mathrm{Fe\text{-}Fe}}$ (meV)	$\mathcal{J}_{R\text{-}\mathrm{Fe}}$ (meV)	D (meV Å^2)	
TbFe_2	0.75	~ 3	-	26	-0.95	-	
HoFe_2	0.75	4.7	16.6	26	-0.43	~ 280	
ErFe_2	0.75	3.6	8.8	30	-0.32	280	
UFe_2	0.27 (fixed)	0.72(2)	0.30(5)	103(5)	$-0.10(3)$	440(30)	model 1
	0.27 (fixed)	0.56(1)		50 (fixed)	$-0.68(3)$		model 2

$\mathcal{J}_{\mathrm{U\text{-}Fe}}$, and $\mathcal{J}_{\mathrm{Fe\text{-}Fe}}$. As noted earlier, we cannot fit these uniquely with one curve. We fix $S_{\mathrm{Fe}}=0.27\mu_B$. Two fits are shown in Fig. 8 and the parameters given in Table III. The first (solid line in Fig. 8) is the best from the viewpoint of χ^2, but it gives both S_{U} and $\mathcal{J}_{\mathrm{Fe\text{-}Fe}}$ larger than we anticipate. The second fit (dashed lines) in Fig. 8 keeps $\mathcal{J}_{\mathrm{Fe\text{-}Fe}}$ fixed at 50 meV and gives a reasonable value of S_{U}. For any type of acceptable fit, we find that $\mathcal{J}_{\mathrm{Fe\text{-}Fe}}$ is still considerably larger than the value found in the $R\mathrm{Fe}_2$ series (Table III).

Perhaps the most remarkable result of this study is the increase in $\mathcal{J}_{\mathrm{Fe\text{-}Fe}}$, despite the strong reduction of S_{Fe}. We believe this is a direct consequence of the $5f-3d$ electron hybridization. This increase in $\mathcal{J}_{\mathrm{Fe\text{-}Fe}}$ may be seen more directly by analyzing the low-q spin-wave regime. Figure 9 presents an analysis in terms of Eq. (3) $E_2=\Delta E_2+Dq^2$, at small q. A dipole-dipole interaction, expressed as a modification of Eq. (3) to give $E=Dq^2(1-q^2)$ was considered by Collins *et al.*[31] in the case of Fe, but the accuracy of our data and the limited q range does not merit such an analysis. As expected, this analysis confirms the large value of $\mathcal{J}_{\mathrm{Fe\text{-}Fe}}$ deduced earlier. The D values are given in Table III.

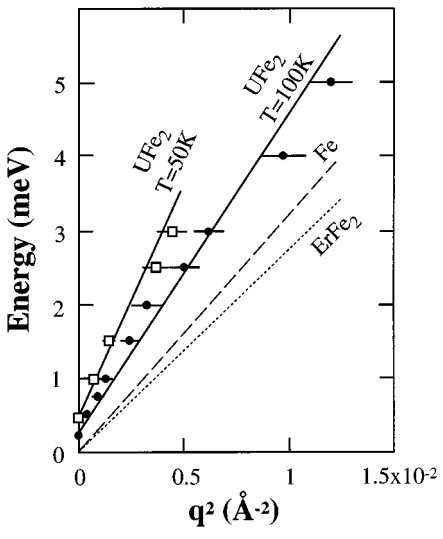

FIG. 9. Analysis of the low **q** region for various materials. Dashed line is best fit to Collins data (Ref. 29) giving $D=325$ (10) meV Å^2 for pure Fe. The dotted curve corresponds to $D=280$ meV Å^2 as given by Refs. 2, 5, and 6 for ErFe_2 at 295 K. The gap is suppressed in presenting this value of D. The two solid lines are fits to UFe_2 at 100 and 50 K where D values of 440 (30) and 630 (50) meV Å^2, respectively, are found.

VI. PHONONS AND MÖSSBAUER EFFECT

A. Phonon spectra

The anomalies in the elastic constants and magnetostriction make the phonons in UFe_2 of particular interest. Furthermore, in searching for the ''missing'' modes in this material it became important to identify excitations, and we have made a rather complete study of phonon modes below 20 meV. The phonon dispersion curves of UFe_2 are shown in Fig. 10. The phonons show a strong similarity to those of LaAl_2 and CeAl_2,[32] with a suitable renormalization due to the heavier U and Fe atoms, although in a detailed comparison of the phonons at the zone-center point there does seem some difficulty in deriving the frequencies with the model used of the $R\mathrm{Al}_2$ compounds.[33] More optic modes exist above 20 meV. In this study we have not made an effort to fit the phonon frequencies with a model, our object being to identify the phonon modes in our search for magnetic modes. As can be seen from Figs. 3 and 7, the phonons are sufficiently strong in UFe_2 that they can be observed at small Q. An alternative way of saying this, of course, is that the magnetism is weak.

The phonon modes show little T dependence, with one noticeable exception. The transverse acoustic [100] phonon softens considerably with temperature. Figure 11(a) presents

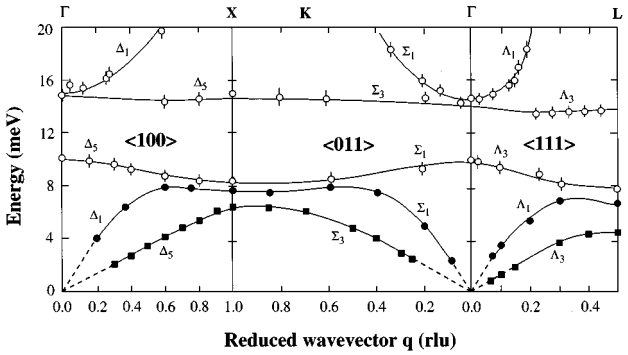

FIG. 10. Complete phonon dispersion curves below 20 meV of UFe_2 at $T=300$ K. The dashed lines at low q correspond to values derived by taking the elastic constants determined by ultrasonic experiments (Ref. 19). The lines are guides to the eye. The open points are from PRISMA, the solid ones are from DN1, Siloë.

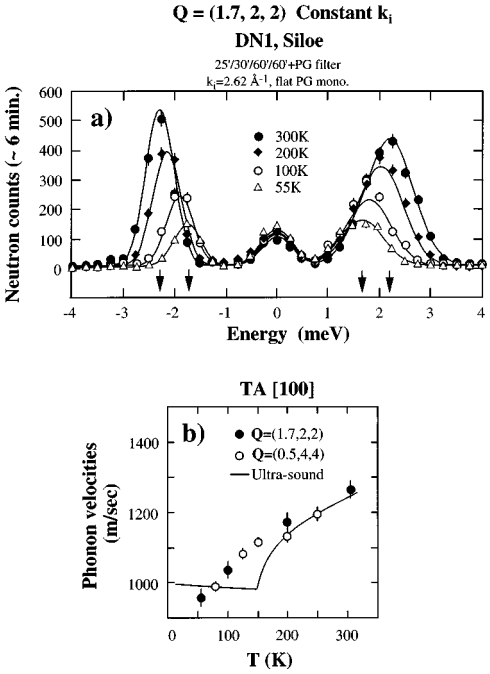

FIG. 11. (a) Constant $\mathbf{Q}=(1.7,2,2)$ showing the softening of the transverse [100] acoustic phonon as a function of temperature. The data are corrected by the $(k_f^3 \cot\theta)$ term necessary when using a constant k_i configuration. The fits are Gaussian curves fixed at the instrumental full width at half maximum. A small incoherent contribution at $E=0$ is also included. After fitting the $T=300$ K data, the intensity for data taken at lower temperature is determined by the corresponding factor; the only parameter in the fits at lower temperatures is thus the frequency of the phonon. The two arrows indicate the energy shift between 300 and 55 K. This figure also shows the absence of any magnetic scattering in this energy range; the Fe mode (2) is well outside this range. (b) Temperature dependence of the TA phonon velocity as deduced from the ultrasound (Ref. 19) (solid line) and neutron experiments at finite $\mathbf{q}$ values (data points).

a series of scans around the (222) zone center at $\mathbf{q}=[0.3,0,0]$ and shows how the transverse acoustic phonon softens with decreasing temperature. The extrapolated slope of the dispersion curve, which gives the phonon velocity, is shown as a function of temperature in Fig. 11(b) and compared with the results deduced from ultrasonic measurements[19] of the c_{44} elastic constant. Although the magnitudes of the phonon velocities given by the two measurements are very similar, the neutron experiments do not see the sharp discontinuity observed in the elastic constant data. We can only suggest that this is a consequence of the different q regimes probed by the two experiments.

The strong reduction (by ~30%) in the phonon velocities connected with the transverse acoustic [100] phonon is further evidence of a strong magnetoelastic interaction. This contributes to the anisotropy, but there is an equally large, but of the opposite sign, term in the single-ion (intrinsic) anisotropy. The result, as discussed earlier, is a small total anisotropy in UFe_2.[17]

B. Mössbauer-effect anomaly

McGuire *et al.*[21] reported an unusual effect in the study UFe_2 with the Fe Mössbauer resonance. At T_C there is an

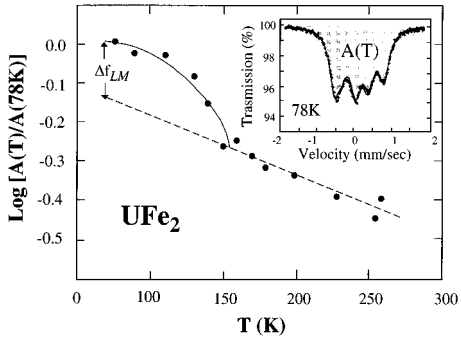

FIG. 12. Lamb-Mössbauer factor (area under the Mössbauer resonance, see inset) as a function of temperature from UFe_2 using the ^{57}Fe Mössbauer resonance (taken from Ref. 21).

abrupt increase in the Lamb-Mössbauer factor (area under the curve of the Mössbauer resonance), and we show this in Fig. 12. There is a different behavior for UFe_2 compared to the other RFe_2 systems. Physically what this means is that at T_C there is a decrease in the mean-square displacement of the Fe atoms, which does not appear to be the case in the RFe_2 compounds.

In developing a theory to explain this effect Eremenko *et al.*[20] have considered three possible explanations. These involve a magnetostrictive compression, a strong Fe-Fe magnetic exchange, and a magnon-phonon interaction. The measurements of the unit cell parameter below T_C eliminate the first possibility. In considering the exchange interaction Eremenko *et al.*[20] concluded that with a T_C of ~167 K and a Fe moment of $0.6\mu_B$ a simple Heisenberg model suggests a $\mathcal{J}_{\text{Fe-Fe}}$~4 meV, and this would be insufficient to influence the Fe vibrational amplitudes. They, therefore, proposed the third solution, a strong magnon-phonon interaction with the acoustic phonons.

Our measurements show two important differences that must be taken into account in reapplying the theory of Ref. 20. First, we have found no evidence for any magnon-phonon interaction, but, second, we have found that the Fe-Fe exchange, $\mathcal{J}_{\text{Fe-Fe}}$, is actually larger than found in the RFe_2 systems. Whether, this exchange interaction is, by itself, large enough to explain the anomalous Lamb-Mössbauer shift in UFe_2 as compared to that found in the other RFe_2 compounds, will require a more careful examination of the theory of Ref. 20.

VII. DISCUSSION

There are two remarkable results emerging from the present study of a strongly hybridized U $5f$ system.

(1) The first is the large Fe-Fe exchange $\mathcal{J}_{\text{Fe-Fe}}$ (or equivalently the large spin-wave stiffness constant D) deduced from the Fe spin-wave mode. To our knowledge, it is unprecedented that diluting Fe results in a larger Fe-Fe exchange. One can show that by taking the distribution of the $3d$ electrons and reducing the interatomic spacing of the Fe atoms from elemental Fe (2.8 Å) to that in UFe_2 (2.5 Å) the value of $\mathcal{J}_{\text{Fe-Fe}}$ should increase[34] by about 20%, but this would be offset by the reduction of coordination from 8 to 6 in going from the element to the compound. The *increase* in $\mathcal{J}_{\text{Fe-Fe}}$ must surely come from the $5f$-$3d$ interaction. Unfor-

tunately, our study of UFe_2 introduces two further aspects. (a) The reduction of the iron moment from 2.2 to $0.6\mu_B$ reduces T_C since, in the simplest of theories, this is proportional to $\mathcal{J}\times S^2$, where $\mathcal{J}$ is the exchange constant, and S the spin value. (b) The strong reduction of $\mathcal{J}_{\text{Fe-Fe}}$ (or D) with temperature. This is not found in either Fe (Ref. 29) or the RFe_2 systems,[6] nor is it accounted for in linear spin-wave theory. Such a strong T dependence shows that nonlinear effects, arising from the interaction between two or more magnons, or between magnons and electrons, destroy the Fe-Fe exchange, and hence drastically lower T_C. The strong temperature dependence of D shows that this simple formula that $T_C \propto \mathcal{J}\times S^2$ cannot be used because $\mathcal{J}$ is itself temperature dependent. The strong decrease in magnetization as a function of temperature was also measured in the bulk magnetization by Aldred.[15] He ascribed this to strong interaction with the Stoner, or single-particle excitations. He suggested that $\sim$40% of the change in magnetization with temperature is due to the magnetization term, and $\sim$60% from the Stoner excitations. Since we have not observed the Stoner modes directly, we do not wish to speculate further on this analysis. We do stress, however, that other independent measurements found an unusual T dependence of the magnetic properties in UFe_2.

(2) The second point is the absence of any scattering involving the uranium spins. Our exhaustive searches below 10 meV eliminate the possibility that a sharp spin-wave response exists in this energy range. Our expectations from the gap in the Fe spin-wave mode is that the acoustic mode, which involves uranium spins [(1) in Fig. 2], lies below the Fe spin wave (see Fig. 8) so this is most puzzling. Of course, a simple solution to this conundrum of the missing modes is to note that the total U moment (see Table I) is almost zero so that the total spin-wave response might only be from Fe, much as it would be in YFe_2, for example. However, this argument is untenable. In spin-wave theory it is the spin, not the total moment, that is important, together with the selection rules for the cross section, and the spin on uranium is finite. From a simple perspective, although mode (3) might be at high energy and weak, we would expect the acoustic mode (1) to have roughly the same intensity as Fe-only spin wave, mode (2).

Two important effects arise from the magnetism of the U $5f$ states: (a) the gap shown in Fig. 6 and (b) the increase in the Fe spin-wave stiffness constant D [see Eq. (2)]. If the spin on the uranium site was zero, there would be no spin-wave gap, or it would be as small as found in pure iron. The only solution we can propose for the absence of, in particular, the acoustic mode is that the spin wave is so strongly broadened that the intensity cannot be observed with a triple-axis spectrometer. Given the tendency for uranium spin waves to broaden with hybridization[35] this is a reasonable hypothesis, although perhaps unsatisfactory from an experimentalist's viewpoint.

Our measurements have further elucidated the magnetoelastic coupling in UFe_2 and the unusual effect observed with Mössbauer spectroscopy. More work should be done also on the phonon spectrum.

Further experiments on UFe_2 would be interesting. For example, to extend the observation of the Fe-spin-wave mode to higher energy to observe the interaction with the Stoner modes. Time-of-flight experiments on polycrystalline samples might be able to observe the density of states arising from the ''missing'' modes, although the strong phonon scattering makes these experiments difficult. $CeFe_2$ represents an interesting material for inelastic studies. We might expect the dynamic behavior to be ''midway'' between the RFe_2 situation and that we have discovered for UFe_2. Recent Compton scattering experiments[36] have confirmed that the total moment on the Ce is small and gone someway to resolving the different numbers in the literature, and experiments to search for the Fe mode and the gap ΔE_2 would be interesting. We are making attempts to grow suitable crystals of $CeFe_2$.

ACKNOWLEDGMENTS

L.P. thanks the European Commission for a HCM Bursary, during which period this work was performed. We thank Mike Brooks of Karlsruhe for a number of illuminating discussions and comments on the manuscript, and Paul Burlet of CEN-Grenoble for advice on the experiments. G.L. thanks the Physics Department of BNL for hospitality and partial support during stays at BNL. Part of the neutron scattering experiments were performed at the DR3 reactor at Risø National Laboratory, and supported by the European Commission through the Large Installation Plan. Work performed at Brookhaven is supported by the US DOE under Contract No. DE-AC02-CH7600016.

[1] R. M. Nicklow, N. C. Koon, C. M. Williams, and J. B. Milstein, Phys. Rev. Lett. **36**, 532 (1976).

[2] J. J. Rhyne, N. C. Koon, J. B. Milstein, and H. A. Alperin, Physica B **86-88**, 149 (1977).

[3] J. J. Rhyne and N. C. Koon, J. Appl. Phys. **49**, 2133 (1978).

[4] N. C. Koon and J. J. Rhyne, Solid State Commun. **26**, 540 (1978).

[5] N. C. Koon and J. J. Rhyne, in *Crystalline Electric Field and Structural Effects in f-Electron Systems*, edited by J. E. Crow, R. P. Guertin, and T. W. Mihalisin (Plenum, New York, 1980), pp. 125–140.

[6] K. Clausen, J. J. Rhyne, B. Lebech, and N. C. Koon, J. Phys. C **15**, 3587 (1982).

[7] J. J. Rhyne, J. Magn. Magn. Mater. **70**, 88 (1987).

[8] A. E. Clark, in *Ferromagnetic Materials*, edited by E. P. Wohlfarth (North-Holland, Amsterdam, 1980), Vol. 1, p. 397.

[9] M. S. S. Brooks, T. Gasche, S. Auluck, L. Nordström, L. Severin, J. Trygg, and B. Johansson, J. Appl. Phys. **70**, 5972 (1991).

[10] J. Jensen and A. Mackintosh, *Rare-Earth Magnetism* (Clarendon Press, Oxford, 1991).

[11] H. H. Hill, in *Plutonium and Other Actinides*, edited by W. N. Miner (Metal. Soc. AIME, New York, 1970), p. 2.

[12] O. Eriksson, L. Nordström, M. S. S. Brooks, and B. Johansson, Phys. Rev. Lett. **60**, 2523 (1988).

[13] S. J. Kennedy, P. J. Brown, and B. R. Coles, J. Phys.: Condens. Matter. **5**, 5169 (1993).

[14] J. Ph. Schillé, F. Bertran, M. Finazzi, Ch. Brouder, J. P. Kappler,

and G. Krill, Phys. Rev. B **50**, 2985 (1994).
[15] A. T. Aldred, J. Magn. Magn. Mater. **10**, 42 (1979).
[16] A. V. Andreev, A. V. Deryagin, R. Z. Levitin, A. S. Markosyan, and M. Zeleny, Phys. Status Solidi A **52**, K13 (1979).
[17] Y. F. Popov, R. Z. Levitin, M. Zaleny, A. V. Deryagin, and A. V. Andreev, Sov. Phys. JETP **51**, 1223 (1980).
[18] K. P. Belov, G. I. Kataev, R. Z. Levitin, S. A. Nikitin, and V. I. Sokolov, Sov. Phys. Usp. **26**, 518 (1983).
[19] T. P. Sorokina, G. M. Kvashnin, and A. M. Kapitonov, Phys. Met. Metallogr. **66**, 164 (1988).
[20] V. V. Eremenko, N. E. Kaner, and V. D. Chercherskii, Sov. Phys. JETP **67**, 241 (1988).
[21] T. K. McGuire and R. H. Herber, Solid State Commun. **48**, 393 (1983).
[22] M. S. S. Brooks, O. Eriksson, B. Johansson, J. J. M. Franse, and P. H. Frings, J. Phys. F **18**, L33 (1988).
[23] M. Wulff, G. H. Lander, B. Lebech, and A. Delapalme, Phys. Rev. B **39**, 4719 (1989).
[24] B. Lebech, M. Wulff, G. H. Lander, J. Rebizant, J. C. Spirlet, and A. Delapalme, J. Phys.: Condens. Matter **1**, 10 299 (1989).
[25] G. H. Lander, M. S. S. Brooks, and B. Johansson, Phys. Rev. B **43**, 13 672 (1991).
[26] O. Eriksson, M. S. S. Brooks, and B. Johansson, Phys. Rev. B **41**, 9087 (1990).
[27] A. Castets, D. Gignoux, and B. Hennion, Phys. Rev. B **25**, 337 (1982).
[28] N. C. Koon and J. J. Rhyne, Phys. Rev. B **23**, 207 (1981).
[29] K. Ibel, *Guide to Neutron Research Facilities at the ILL* (Institut Laue Langevin, Grenoble, France, 1994), p. 94.
[30] U. Steigenberger, M. Hagen, R. Caciuffo, F. Cilloco, and K. Sachetti, Nucl. Instrum. Methods B **53**, 87 (1991).
[31] M. F. Collins, V. J. Minkiewicz, R. Nathans, L. Passell, and G. Shirane, Phys. Rev. **179**, 417 (1969); M. W. Stringfellow, J. Phys. C **1**, 950 (1969).
[32] C. T. Yeh, W. Reichardt, B. Renker, N. Nücker, and M. Loewenhaupt, J. Phys. (Paris) Colloq. **42**, C6-371 (1981); W. Reichardt and N. Nücker, J. Phys. F **14**, L135 (1984).
[33] W. Reichardt (private communication).
[34] R. B. Griffiths, Phys. Rev. **124**, 1023 (1961).
[35] W. J. L. Buyers and T. M. Holden, in *Handbook of the Physics and Chemistry of the Actinides*, edited by A. J. Freeman and G. H. Lander (North-Holland, Amsterdam, 1985), Vol. 2, p. 239.
[36] M. J. Cooper, P. K. Lawson, M. A. G. Dixon, E. Zukowski, D. N. Timms, F. Itoh, H. Sakurai, H. Kawata, Y. Tanaka, and M. Ito (unpublished).